

# Indole-2-Carboxamide Derivative LG25 Inhibits Triple-Negative Breast Cancer Growth By Suppressing Akt/mTOR/NF- $\kappa$ B Signalling Pathway

This article was published in the following Dove Press journal:  
*Drug Design, Development and Therapy*

Xiaohong Xu<sup>1</sup>  
Vinothkumar Rajamanickam<sup>1</sup>  
Sheng Shu<sup>1</sup>  
Zhouli Liu<sup>1</sup>  
Tao Yan<sup>1</sup>  
Jinxin He<sup>1</sup>  
Zhiguo Liu<sup>1</sup>  
Guilong Guo<sup>2</sup>  
Guang Liang<sup>1</sup>  
Yi Wang<sup>1</sup> 

<sup>1</sup>Chemical Biology Research Center, School of Pharmaceutical Sciences, Wenzhou Medical University, Wenzhou, Zhejiang 325035, People's Republic of China; <sup>2</sup>Department of Surgical Oncology, The First Affiliated Hospital of Wenzhou Medical University, Wenzhou, Zhejiang 325000, People's Republic of China

**Background:** Triple-negative breast cancer (TNBC) is an aggressive subtype of breast cancer which is associated with poor patient outcome and lack of targeted therapy. Our laboratory has synthesized a series of indole-2-carboxamide derivatives. Among this series, compound LG25 showed a favorable pharmacological profile against sepsis and inflammatory diseases. In the present study, we investigated the chemotherapeutic potential of LG25 against TNBC utilizing in vitro and in vivo models.

**Methods:** Changes in cell viability, cell cycle phases and apoptosis were analyzed using MTT, clonogenic assay, FACS and Western blotting assays. The anti-cancer effects of LG25 were further determined in a xenograft mouse model.

**Results:** Our findings reveal that LG25 reduced TNBC viability in a dose-dependent manner. Flow cytometric and Western blot analyses showed that LG25 enhances G2/M cell cycle arrest and induced cell apoptosis. In addition, LG25 treatment significantly inhibited Akt/mTOR phosphorylation and nuclear translocation of nuclear factor- $\kappa$ B (NF- $\kappa$ B). These inhibitory activities of LG25 were confirmed in mice implanted MDA-MB-231 TNBC cells.

**Conclusion:** Our studies provide experimental evidence that indole-2-carboxamide derivative LG25 effectively targeted TNBC in preclinical models by inducing cell cycle arrest and apoptosis, through suppressing Akt/mTOR/NF- $\kappa$ B signaling pathway.

**Keywords:** indole analog, triple-negative breast cancer, cell cycle arrest, apoptosis, Akt, mTOR

## Introduction

Breast cancer (BC) is one of the most prevalent malignant tumors and the leading cause of cancer-related deaths among women worldwide. Generally, breast cancer can be divided into four main categories based on the different gene expression signatures. These include estrogen receptor (ER) positive, progesterone receptor (PR) positive, human epidermal growth factor receptor 2 (HER2) positive, and triple-negative breast cancer (TNBC).<sup>1</sup> Typically, TNBC is characterized by the absence of ER/PR and a lack of overexpressed HER2, and therefore, recalcitrant to either hormonal therapy or anti-HER2 agents. Epidemiological studies reveal that TNBC alone accounts for 15–20% of all breast cancer cases.<sup>2</sup> Chemotherapy remains the standard treatment of TNBC.<sup>3</sup> Nevertheless, TNBC patients with residual disease after chemotherapy show a high rate of recurrence and a low 3-year survival rate.<sup>4</sup> In addition, compared to the hormone receptor-positive subtypes, TNBC is associated with a higher mortality rate due to aggressive lung and brain metastasis.<sup>4–6</sup> To date, no targeted therapies have been

Correspondence: Yi Wang  
Chemical Biology Research Center,  
School of Pharmaceutical Sciences,  
Wenzhou Medical University, Wenzhou,  
Zhejiang 325035, People's Republic of  
China  
Tel/Fax +8657785773060  
Email yi.wang1122@wmu.edu.cn

approved for the treatment of TNBC, underscoring the urgent need to discover new agents.

Genetic alterations in signaling pathways may cause abnormal cell growth, disrupted cell cycle progression, and dysregulated apoptotic responses, which are hallmarks of cancer.<sup>7,8</sup> The phosphatidylinositol-3-kinase (PI3K)/Akt and the mammalian target of rapamycin (mTOR) signaling pathways regulate a variety of cellular processes, including cell proliferation and cell cycle progression. Therefore, the PI3K/Akt pathway is directly related to quiescence, proliferation, cancer development, and longevity.<sup>9–12</sup> Aberrations in the Akt/mTOR signaling pathway promotes oncogenic events in many cancers, including TNBC.<sup>13</sup> Thus, agents targeting Akt/mTOR pathway are promising for TNBC.

Natural products exert a broad range of biological activities and are gaining attention in the prevention and treatment of various diseases including cancer.<sup>14</sup> Most natural products contain indole such as indole terpenoids<sup>15</sup> and indole alkaloids.<sup>16</sup> In addition, indole is the major structural component of several clinically used drugs. We previously synthesized a novel class of indole derivatives, which exhibited excellent activity against lipopolysaccharide (LPS)-stimulated inflammatory responses in macrophages and LPS-induced sepsis in mice.<sup>17</sup> Among this series, compound 14f (Figure 1A), which is renamed as LG25 in this study, showed strong inhibitory effect on interleukin-6 (IL-6) and tumor necrosis factor- $\alpha$  (TNF- $\alpha$ ) induction.<sup>17</sup> Since it is well known that inflammation promotes the development of solid tumors.<sup>18</sup> To build on our previous studies, we investigated whether LG25 was effective against TNBC cells as well as MDA-MB-231 xenograft mice model, owing to its potent anti-inflammatory activities.

## Materials And Methods

### Chemicals And Reagents

The indole-2-carboxamide derivative, 5-(furan-2-carboxamido)-N-(4-(4-methylpiperazin-1-yl)phenyl)-1-(4-(trifluoromethyl)benzyl)-1H-indole-2-carboxamide (LG25), was synthesized as described by us previously.<sup>17</sup> The chemical structure of LG25 is shown in Figure 1A. Paclitaxel (PTX) was purchased from Aladdin (Shanghai, China). Cell viability was measured through the MTT assay (3-(4,5-dimethylthiazol-2-yl)-2,5-diphenyl-2 tetrazolium bromide) (Beyotime Biotech, Nantong, China). Hoechst 33258 staining solution was also obtained from Beyotime Biotech. Annexin V-FITC/Propidium Iodide apoptosis and PI/RNase

cell cycle detection kits were purchased from BD Biosciences (Franklin Lakes, NJ). Antibodies against mouse double minute 2 (MDM-2), cyclin-dependent kinase 1 (CDC2), Cyclin B1, and horseradish peroxidase (HRP)-conjugated secondary antibodies were purchased from Santa Cruz Biotechnology (Santa Cruz, CA). Antibodies against p53, B cell lymphoma 2 (Bcl-2), Bcl-2-associated protein X (Bax), phosphorylated (p)-mTOR, p-Akt, Akt, phosphorylated ribosomal protein 6 (p-S6RP), NF- $\kappa$ B p65 subunit, inhibitor of  $\kappa$ B (I $\kappa$ B- $\alpha$ ), and GAPDH were obtained from Cell Signaling Technology (Danvers, MA). Anti-Ki67 antibody was from Abcam (Cambridge, UK). Matrigel was purchased from BD Biosciences (Franklin Lakes, NJ).

### Breast Cancer Cell Lines And Cell Culture

TNBC cell lines MDA-MB-231 and BT-549 were obtained from the Cell Bank of Shanghai Institutes for Biological Sciences (Shanghai, China). MDA-MB-231 cells were cultured in DMEM containing high glucose (Gibco, Eggenstein, Germany) and BT-549 cells were cultured in RPMI-1640 medium (Gibco). Both growth media formulations were supplemented with 10% fetal bovine serum (FBS) (Gibco) and 100 U/mL of penicillin and 100  $\mu$ g/mL streptomycin (Gibco).

To assess cell viability, MDA-MB-231 and BT-549 cells were seeded at a density of  $5 \times 10^3$  cells/well in 96-well plates. Cells were allowed to adhere overnight. Cells were then exposed to increasing concentrations of LG25 for 24 hrs. The tested concentrations included 0.5, 0.75, 1.0, 1.25, 2.5, 5 and 10  $\mu$ M LG25. DMSO was used as vehicle control. Following treatments, MTT reagent was added at a final concentration of 1 mg/mL. Cell viability was determined by measuring absorbance at 490 nm using SpectraMax iD3 microplate reader (Molecular Devices, San Jose, CA).

Apoptosis was determined using Annexin V-FITC/PI apoptosis labeling. Briefly, MDA-MB-231 and BT-549 cells were seeded at a density of  $3 \times 10^5$  cells per well in 6-well plates. Cells were treated with LG25 at 1.25, 2.5 or 5  $\mu$ M, PTX at 5  $\mu$ M, or DMSO for 24 hrs. Cell suspension was then prepared and stained with FITC-conjugated anti-Annexin V and PI. Apoptosis was detected using FACSCalibur flow cytometer (BD Biosciences). Data were analyzed using FlowJo 7.6 (Ashland, OR). To determine cell cycle phase, cells were treated as for apoptosis detection. However, treatments were only carried out for 16 hrs. Cells were harvested and fixed in ice-cold 75% ethanol following treatments. DNA



was labeled with PI/Rnase staining buffer (BD Biosciences) for 20 mins in the dark at 4°C. Distribution of cell cycle phases was analyzed using BD FACSCalibur.

## Colony Formation And Migration Assays

MDA-MB-231 and BT-549 cells were seeded at a density of  $1 \times 10^3$  cells/well in 6-well plates. Cells were allowed to adhere overnight and were then treated with LG25 at various concentrations, PTX at 5  $\mu$ M, or DMSO vehicle control for 12 hrs. Following treatments, cells were washed three times with PBS and cultured in treatment-free medium for 15 days. Emerging colonies were stained with crystal violet and counted. All experiments were conducted at least three times.

To test the effect of LG25 on TNBC migration, we performed scratch assays in MDA-MB-231 cells. Cells were seeded at a density of  $3 \times 10^5$  cells/well in 6-well plates with complete growth media. At 90% confluency, media were replaced with serum-free medium. Cell monolayer was then scratched using a 200  $\mu$ L pipette tip. Cells were then allowed to migrate for 24 hrs in serum-free media containing LG25 at 0.63, 1.25 or 2.5  $\mu$ M, PTX at 5  $\mu$ M, or DMSO vehicle control. Images were acquired at 0 and 24 hrs. The relative migratory rate was calculated using the following formula: relative migration rate = (distance between gap at 0 hrs – distance between gap at 24 hrs)/distance between gap at 0 hrs  $\times$  100%.

## Western Blotting Analysis

Proteins were isolated from cells and tumor tissues from mice. Protein concentrations were determined using the Bradford assay (Bio-Rad, Hercules, CA). Samples were separated on precast 8–12% SDS polyacrylamide gels. After electrophoresis, proteins were transferred to polyvinylidene difluoride (PVDF) membranes. Membranes were blocked with 5% non-fat milk in tris-buffered saline containing 0.1% Tween 20 (TBST) for 90 mins at room temperature. Then, primary antibodies (1:1000) in TBST were added and membranes were incubated overnight at 4°C. After washing with TBST, HRP-conjugated secondary antibodies (1:3000) were added for 1 hrs at room temperature. The immunoreactive bands were visualized by using ECL kit (Bio-Rad) and analyzed using Image J (National Institute of Health, Bethesda, MD).

## In Vivo Xenograft Mouse Model

Eight-week old female BALB/c nude mice, weighing 20–22 g, were purchased from Shanghai Laboratory Animal Center

(Shanghai, China). Mice were housed at a constant room temperature with a 12/12-h light/dark cycle and fed a standard rodent diet and water. All animal experiments complied with the Wenzhou Medical University Policy on the Care and Use of Laboratory Animals (Approved documents: wyd2014-0059). MDA-MB-231 cells were injected subcutaneously into the right flank of each mouse at the density of  $5 \times 10^6$  cells in 0.1 mL Matrigel/PBS (1:1 ratio). Once the tumors reached the volume of 140–160 mm<sup>3</sup>, mice were treated with LG25 at 5 or 10 mg/kg, once daily for 12 days. Control mice received 100  $\mu$ L of ethoxylated castor oil as vehicle control. The bodyweights of mice were recorded. Tumor volumes were determined by measuring length (l) and width (w) and calculating volume as  $0.5 \times l \times w^2$ , at the indicated time points. At the end of the treatment period, mice were anesthetized with 3.5% isoflurane and euthanized in a CO<sub>2</sub> chamber.

The harvested tumor tissues from mice were fixed in 10% formalin, processed and embedded in paraffin. Paraffin-embedded tissues were sectioned at the thickness of 5  $\mu$ m. Tissue sections were stained with Ki67 antibody to assess cell proliferation. HRP-conjugated secondary antibody and chromagen staining were used to detect immunoreactivity.

## Statistical Analysis

All data were obtained from at least 3 independent experiments. Values from quantitative experiments are expressed as the mean  $\pm$  SEM. All statistical analyses were performed using GraphPad Pro 7.0 (GraphPad, San Diego, CA). Significance was determined using one-way analysis of variance (ANOVA) followed by a Tukey's post hoc analysis. A value of  $P < 0.05$  was considered statistically significant.

## Results

### LG25 Reduces TNBC Cell Viability And Migration

We first investigated the potential cytotoxic effects of LG25 on MDA-MB-231 and BT-549 cells. To do this, we performed MTT viability assay following exposure of TNBC cells to various concentrations of LG25 for 24 hrs. Our results show that LG25 reduced viability of TNBC cells with an IC<sub>50</sub> of  $1.22 \pm 0.10$   $\mu$ M for MDA-MB-231 cells and  $1.28 \pm 0.02$   $\mu$ M for BT-549 cells (Figure 1B). We then performed colony formation assays to determine whether LG25 reduces cell survival and colony-forming abilities of TNBC. For these studies, we used Paclitaxel (PTX), a chemotherapeutic drug, as the positive control. Our results confirmed that LG25 exerted an inhibitory



effect on TNBC cell survival and this effect was comparable to PTX at the same concentration (Figure 1C). Furthermore, we performed a wound-healing assay to assess the migratory capacity of TNBC and the effect of LG25. As shown in Figure 1D, LG25 treatment significantly inhibited the migratory capacity of MDA-MB-231 cells. We found MDA-MB-231 cells to exhibit a migration rate of  $38.01 \pm 1.13\%$  in DMSO-treated control group. Exposure of MDA-MB-231 cells to increasing concentrations of LG25 yielded migration rates of  $35.72 \pm 4.82\%$  at  $0.63 \mu\text{M}$ ,  $26.03 \pm 0.50\%$  at  $1.25 \mu\text{M}$ , and  $18.14 \pm 1.34\%$  at  $2.5 \mu\text{M}$  LG25 (Supplementary Figure S1). We also found that LG25 at  $2.5 \mu\text{M}$  was more effective in inhibiting the migration of MDA-MB-231 cells compared to  $5 \mu\text{M}$  PTX (migration rate =  $26.62 \pm 6.41\%$ ). Collectively, these results indicate that LG25 reduces TNBC survival and inhibits migratory capacity.

## LG25 Causes Mitotic Cell Cycle Arrest In A Dose-Dependent Manner

Uncontrolled cell proliferation is a feature of cancer cells and is attributed to the loss of cell-cycle control. To identify whether LG25 inhibited TNBC cell growth through induction of cell cycle arrest, we examined the cycle phase in PI-stained MDA-MB-231 and BT-549 cells. Our results show that LG25 caused accumulation of cells in the G2/M phase in a dose-dependent manner (Figure 2A–C). Unlike results of the migration assay, we found LG25 was not as effective as PTX in causing cell cycle arrest in TNBC (54% versus 78%). To confirm these results of cell cycle arrest, we probed key proteins associated with G2/M transition (Figure 2D). These proteins include murine double minute 2 (MDM2, a P53 regulator), cyclin-dependent kinase 1/cell division cycle protein 2 (CDC2), and cyclin B1. Western blot analysis showed decreased levels of MDM-2 (Figure 2E), CDC-2 (Figure 2F), and cyclin B1 (Figure 2G) in cells following exposure to LG25. In summary, these data indicate that LG25 causes cell cycle arrest which may contribute to reduced growth of MDA-MB-231 cells.

## LG25 Induces Apoptotic Cell Death In TNBC Cells

Next, we examined the possible effect of LG25 on inducing cell apoptosis. To do so, we stained cells with Annexin-V and PI following exposure to LG25. Our results presented in Figure 3A–C show that a significant increase in the proportion of early and late apoptotic cells after LG25 treatment. The

inhibitory effect of LG25 was robust at  $5 \mu\text{M}$  concentration, in both TNBC lines (50–53% apoptosis) compared to vehicle-treated control cells. However, LG25 at low doses ( $1.25$  and  $2.5 \mu\text{M}$ ) only induced slightly apoptosis in both TNBC cell lines when compared to those of the vehicle control (Figure 3A–C). In comparison, PTX showed an apoptotic index of 10–15% when compared to that of LG25 at the same concentration. We then stained the cells with Hoechst 33258 and confirmed the above findings (Figure S2). To supplement these results with additional measures of apoptosis induction, we measured apoptosis-related proteins by Western blotting. As expected, LG25 increased the levels of BAX and decreased the levels of Bcl-2 (Figure 3D–F). Taken together, our findings indicate that LG25 and PTX exert inhibitory activities against TNBC through cell cycle arrest and induction of apoptosis, although, the contribution of each mechanism may be slightly different.

## LG25 Suppresses Akt/mTOR Phosphorylation And Inactivates NF- $\kappa$ B Signaling Pathway In MDA-MB-231 Cells

To dissect the molecular mechanisms underlying inhibitory activities of LG25 in TNBC, we exposed to the cells to varying concentrations of LG25 and assessed the pro-survival Akt signalling pathway. Our data shows that LG25 reduces the phosphorylation of Akt, mTOR and ribosomal protein S6 (S6RP) in a dose-dependent manner (Figure 4A–D). Since S6RP is a downstream target of the PI3K/Akt/mTOR signaling cascade, phosphorylation of this axis is indicative of active signaling. Studies have also shown that nuclear factor- $\kappa$ B (NF- $\kappa$ B) activity in tumor cells is controlled by Akt and that the ability of mTOR to activate NF- $\kappa$ B in tumor cells is dependent, at least partly, on Akt.<sup>19</sup> Hence, we assessed the status of NF- $\kappa$ B activation in TNBC following treatment with LG25. As shown in Figure 4E–H, LG25 significantly reduced the levels of nuclear NF- $\kappa$ B. LG25 also inhibited the degradation of the inhibitor of  $\kappa$ B (I $\kappa$ B), which is required for NF- $\kappa$ B p65 subunit translocation. These results suggest that LG25 suppresses Akt/mTOR and NF- $\kappa$ B signalling axis to reduce TNBC growth.

## LG25 Reduces TNBC Tumor Growth In Vivo Through Suppressing Akt/mTOR Pathway And Inducing Apoptotic Cell Death

To confirm the results obtained in our culture studies, we implanted MDA-MB-231 in mice and treated the mice with

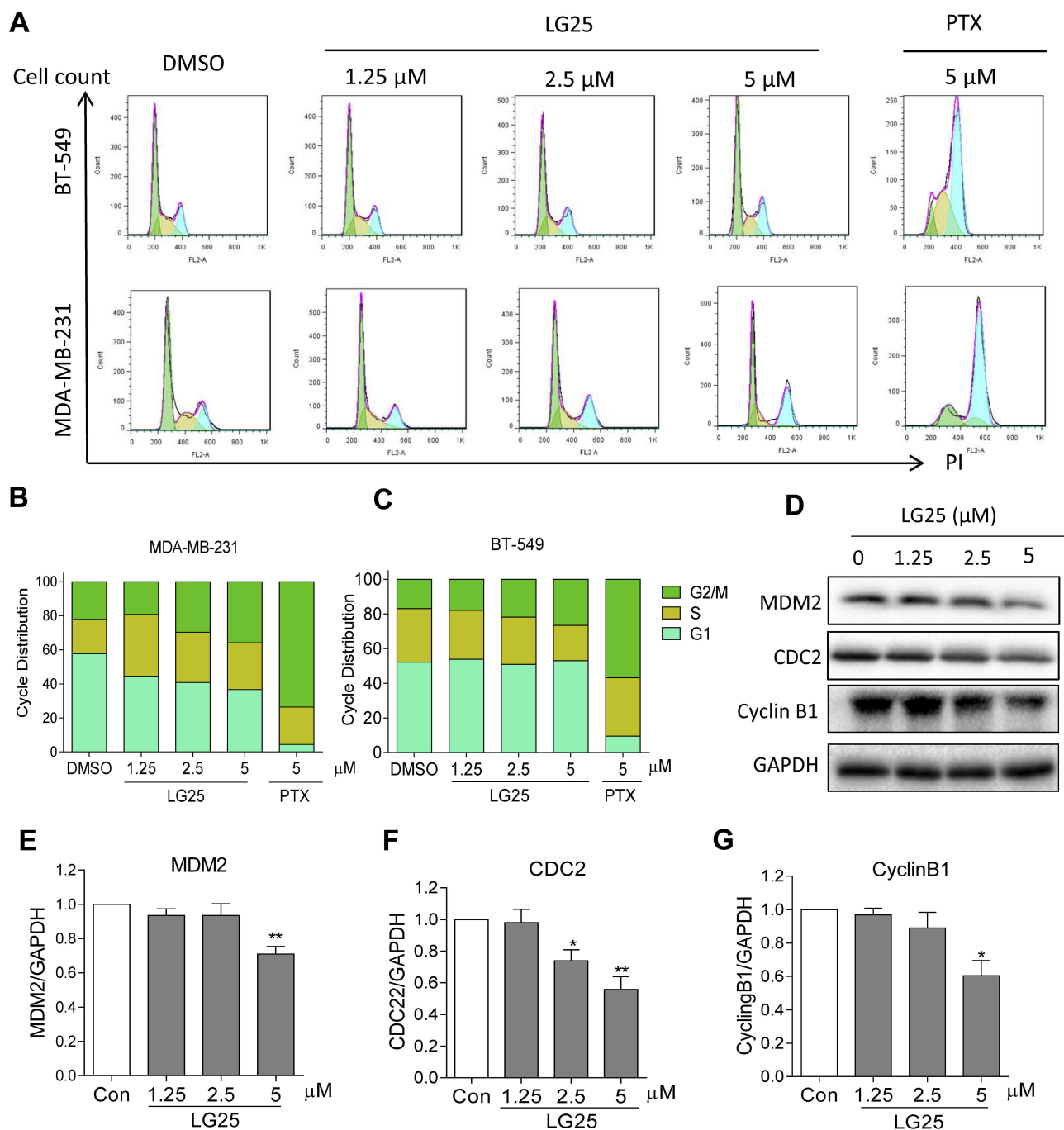


**Figure 2** LG25 causes G2/M cell cycle arrest. **(A)** MDA-MB-231 and BT-549 cells were treated with LG25 at 1.25, 2.5, or 5 μM, paclitaxel at 5 μM, or DMSO vehicle control for 16 hrs. Cell cycle distribution was determined using flow cytometry. Representative images of three independent experiments are shown. The percentage of cells at different cell cycle phases was determined **(B–C)**. **(D)** MDA-MB-231 cells were treated as outlined in panel A. Levels of G2/M-associated proteins MDM-2 **(E)**, CDC-2 **(F)**, and Cyclin B1 **(G)** were determined by Western blotting. GAPDH was used as the loading control. Representative Western blots from three independent experiments and quantitative data were shown. Data were shown as mean ± SEM (n=3). \**P* < 0.05; \*\**P* < 0.01 compared to vehicle control.

LG25. Our results show significantly reduced tumor volumes in mice treated with LG25 compared to vehicle-treated control mice (Figure 5A–C). We also detected activation of the Akt/mTOR pathway in tumor specimens through Western blotting (Figure 5D–F). Levels of Bcl-2, p-mTOR and p-Akt were all markedly reduced by LG25

treatment (Figure 5D–G). Furthermore, the number of Ki-67 positive cells, indicative of cell proliferation, was greatly reduced after LG25 treatment (Figure 5H). Finally, our in vivo data shows that LG25 does not induce any pathological events in vivo as histological assessment of vital organs including the hearts, kidneys and livers of LG25-treated

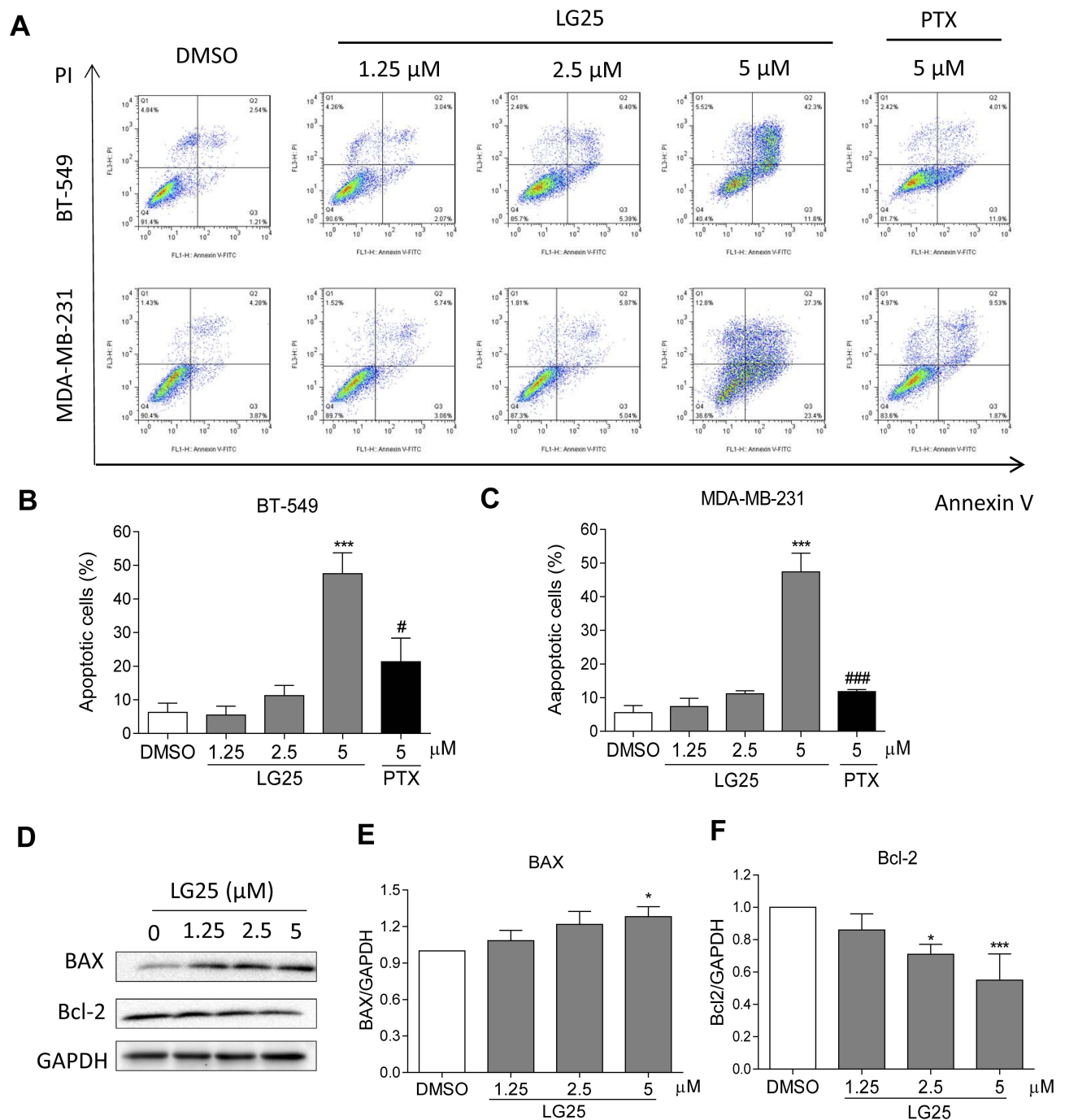


**Figure 3** LG25 induces apoptosis in TNBC cells. **(A)** Induction of early and late apoptosis in TNBC cells was determined by staining cells with Annexin V/PI following treatment with LG25. **(B, C)** Quantification of data shown in panel A. Data presented as means  $\pm$  SEM from three experiments. **(D)** MDA-MB-231 cells were treated with LG25 at 1.25, 2.5 or 5  $\mu$ M, or DMSO vehicle control for 24 hrs. Protein levels of Bcl-2 and Bax were determined by Western blotting. GAPDH was used as loading control. **(E, F)** Densitometric quantification of Western blot data presented in panel D. Data presented as mean  $\pm$  SEM from three experiments. \* $P < 0.05$ ; \*\*\* $P < 0.001$  compared to vehicle control group; # $P < 0.05$ ; ### $P < 0.001$  compared to LG25-5  $\mu$ M treated group.

mice were indistinguishable from vehicle-treated control mice (Figure S3A). The body weights of LG-treated mice were also similar to control mice (Figure S3B). In summary,

these findings demonstrate that LG25 is effective in reducing TNBC tumor growth in vivo and is well tolerated by the animals used in this study.

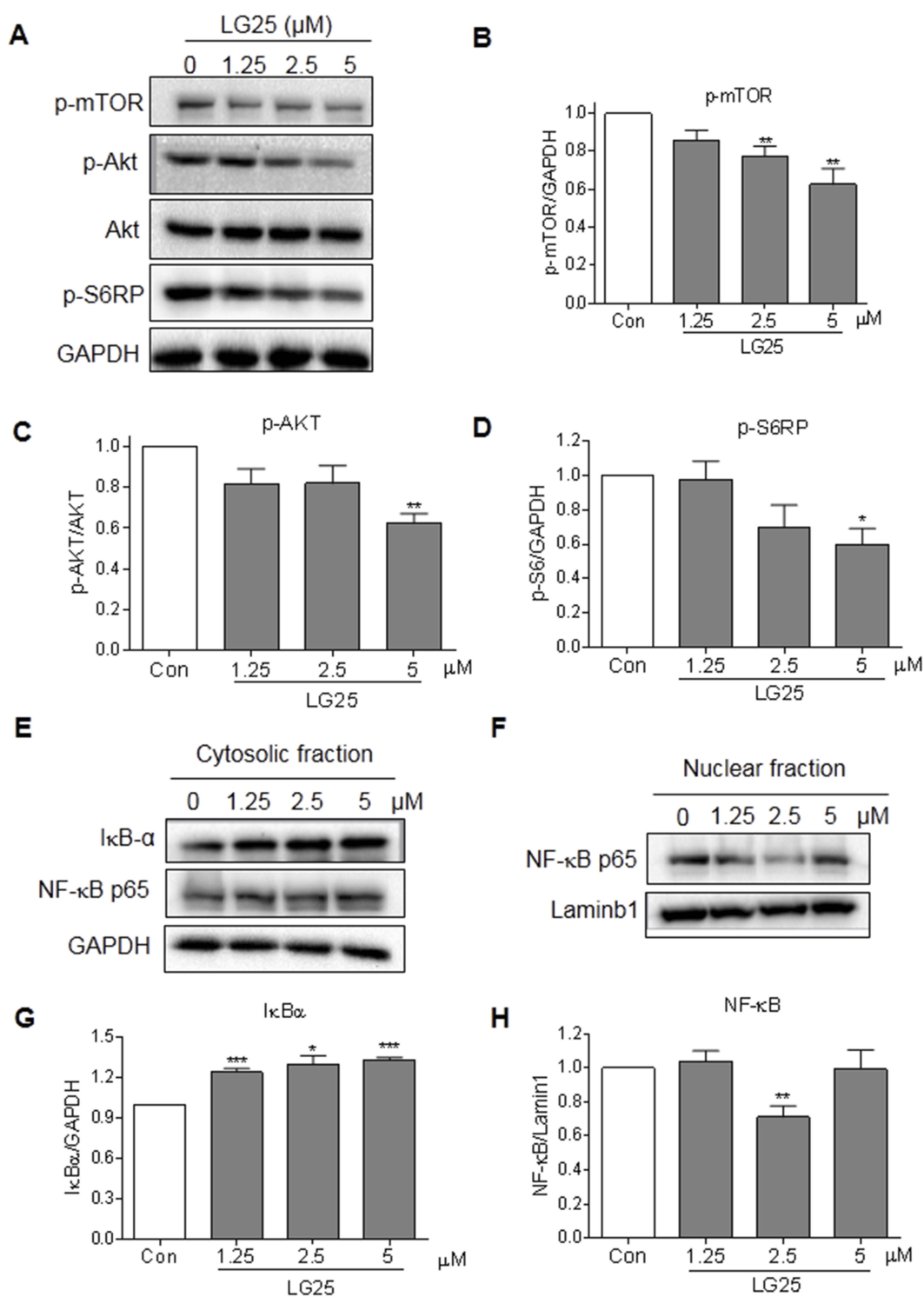


**Figure 4** LG25 inhibited the activation of Akt/mTOR and NF- $\kappa$ B signalling pathways. **(A)** MDA-MB-231 cells were treated with LG25 for 2 hrs. Protein levels of p-mTOR, p-Akt, Akt, and p-S6RP were evaluated by Western blotting. GAPDH was used as the loading control. **(B–D)** Densitometric quantification of p-mTOR, p-Akt, and pS6RP levels. Data presented as mean  $\pm$  SEM from three independent experiments. \* $P$  < 0.05; \*\* $P$  < 0.01 compared to vehicle control group. **(E)** MDA-MB-231 cells were treated with LG25 for 6 hrs. The protein levels of NF- $\kappa$ B and I $\kappa$ B- $\alpha$  in nuclear and cytosolic fractions were evaluated by Western blotting. Laminin B1 was used as loading control for nuclear proteins and GAPDH for cytosolic proteins. **(G–H)** Densitometric quantification of cytosolic I $\kappa$ B and nuclear NF- $\kappa$ B for **(E)** and **(F)**. Data presented as means  $\pm$  SEM from three experiments. \* $P$  < 0.05; \*\* $P$  < 0.01; \*\*\* $P$  < 0.001 compared to vehicle control.



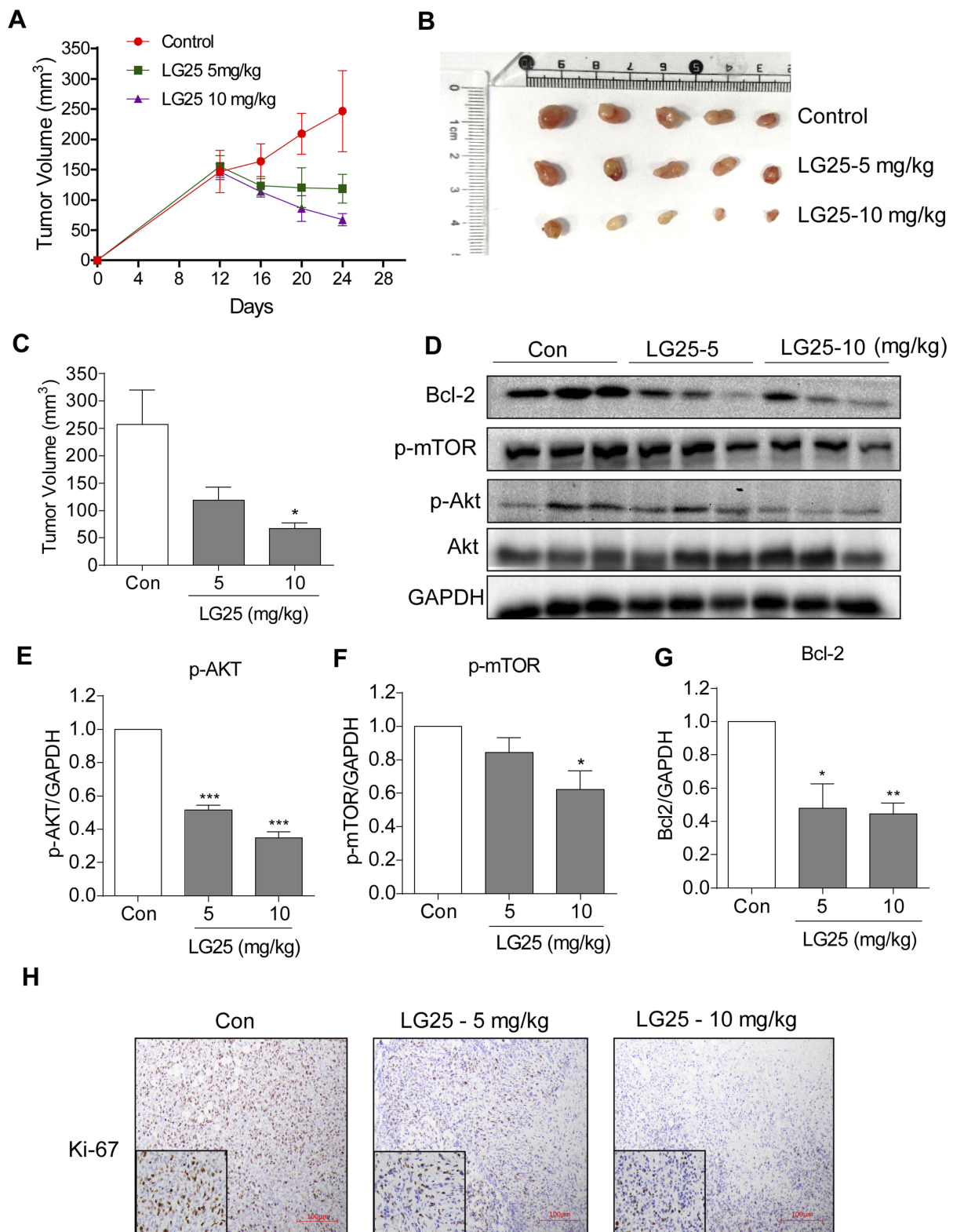


**Figure 5** LG25 inhibited MDA-MB-231 tumor growth in mice by suppressing Akt/mTOR signalling. MDA-MB-231 cells were injected subcutaneously into the right flank of the BALB/c nude female mice. Mice were then treated with LG25 for 12 days. **(A)** Tumour volumes measured at indicated time points in the experimental groups (n=5). **(B)** Image showing harvested tumor specimens at the conclusion of the study (day 24). **(C)** Tumor volumes at the conclusion of the study. Data were presented as mean  $\pm$  SEM (n=5). **(D)** Western blotting analysis of Bcl-2, p-mTOR, and p-Akt protein expression in tumor tissues from mice. GAPDH was used as loading control. **(E–G)** Densitometric quantification of Bcl-2, p-Akt, and p-mTOR. Data are shown as mean  $\pm$  SEM (n=5). \* $P < 0.05$ ; \*\* $P < 0.01$ ; \*\*\* $P < 0.001$  compared to vehicle control group. **(H)** Immunohistochemical staining for Ki67 in tumor tissues (shown as brown). Slides were counterstained with hematoxylin (blue). Representative photos are shown.

## Discussion

Indole, a planar heterocyclic molecule, is the parent substance of a large number of important natural compounds. Indole derivatives have been shown to exert considerable pharmacological activities against viral infections,<sup>20</sup> inflammatory conditions,<sup>17</sup> hyperlipidemia,<sup>21</sup> and tumor growth.<sup>22,23</sup> Previous findings have reported that indole analogues inhibit cancer development and also attenuate various side effects associated with anticancer drugs. For example, Ashok and colleagues reported that novel indole-fused benzo-oxazepines inhibits invasion of hepatocellular carcinoma by targeting interleukin-6 mediated JAK2/STAT3 oncogenic signals.<sup>24</sup> Naga et al revealed that indole-3-carbinol protects against cisplatin-induced acute nephrotoxicity, while enhancing the cytotoxicity of cisplatin.<sup>25</sup> These studies indicate the potential application of indole analogues in chemotherapy. Herein, we investigated the potential antitumor activity of a novel indole compound, LG25, in two TNBC cell lines. Our data shows that LG25 treatment markedly suppressed the proliferation and migration in both MDA-MB-231 and BT-549 cells (Figure 1). These outcomes may have results from a G2/M arrest and induction of apoptosis (Figures 2 and 3). Treatment of mice harboring TNBC with LG25 showed that this indole derivative is effective in reducing tumor growth, potentially by suppressing Akt/mTOR pathway.

Investigation of potential mechanisms underlying the suppression of TNBC growth by LG25 highlighted the involvement of the Akt/mTOR pathway. The PI3K/Akt/mTOR pathway is an important pathway in regulating cellular quiescence, proliferation, and longevity.<sup>26</sup> Genomic instability in the PI3K/Akt/mTOR pathway is common in breast cancer across various subtypes.<sup>27</sup> This signaling pathway is activated by stimulation of receptor tyrosine kinases, which in turn trigger PI3K activation, followed by phosphorylation of Akt and mTOR complex 1 (mTORC1).<sup>26</sup> In TNBC, oncogenic PI3K/Akt/mTOR pathway can be activated through the overexpression of upstream regulators. These regulators include epidermal growth factor receptor, activating mutations of *PI3K* catalytic subunit  $\alpha$ , loss of function or expression of phosphatase and tensin homolog, and the proline-rich inositol polyphosphatase, which are downregulators of PI3K.<sup>26,28–30</sup> In addition, several oncogenic pathways (e.g. FGFR, cMET, RAF) activated by P53 inactivation converge to activate the PI3K pathway.<sup>31</sup> Increased activity of Akt may increase the expression of anti-apoptotic proteins Bcl-2 and MDM2 to evade apoptosis.<sup>13</sup> Elena et al showed that indole-

3-carbinol reduces Akt activity, causing specific alteration to epidermal growth factor receptor and hormone-signaling pathways, which targets androgen-activated gene promoter- and growth factor-responsive genes in human breast cancer cells.<sup>32</sup> In our study, increased phosphorylated Akt and mTOR and increased level of anti-apoptotic Bcl-2 were found in both MDA-MB-231 cells and tumor xenografts (Figures 4A and 5D). However, we found that LG25 treatment decreased p-AKT, p-mTOR and Bcl-2 levels in vitro and in vivo (Figures 4A and 5D), suggested that Akt/mTOR and Bcl-2 pathways may be involved in reducing cell survival and inducing apoptosis. Further studies are certainly warranted to understand how LG25 regulates this Akt/mTOR pathway at molecular level.

A critical protein downstream of Akt is NF- $\kappa$ B, which is known to play a major role in the development of cancers.<sup>33</sup> As a transcription factor, NF- $\kappa$ B also represents an important molecular link between inflammation to cancer, regulating several genes responsible for inhibiting apoptosis and enhancing the progression of the cell cycle, leading to angiogenesis and metastasis.<sup>34</sup> A crosstalk between the mTOR and NF- $\kappa$ B pathways has been reported. Han et al showed that mTOR downstream from Akt controls NF- $\kappa$ B activity in PTEN-null/inactive prostate cancer cells by interaction with and stimulation of IKK (also known as I $\kappa$ Bk, inhibitor of NF- $\kappa$ B kinase).<sup>19</sup> Indeed, mTOR regulates Akt via a feedback mechanism, increasing NF- $\kappa$ B activation, as well as mediating induction of IKK and leading to the activation of NF- $\kappa$ B.<sup>19</sup> Consistent with these reports, our study shows that LG25 blocks the Akt/NF- $\kappa$ B signaling network to regulate cell cycle progression, cell survival, and induction of apoptosis in TNBC (Figure 4E and F). Our preliminary results show that LG25 may have clinical utility against TNBC.

In summary, our study demonstrated that indole-2-carboxamide derivative LG25 inhibited the growth of TNBC cells in pre-clinical models. LG25 caused cytotoxicity in TNBC cells as evident by G2/M cell cycle deregulation and induction of apoptosis. Furthermore, our molecular findings support the hypothesis that LG25 have multifunctional targets which may include Akt/mTOR and NF- $\kappa$ B signaling pathways. The limitation of this study is that we did not measure the effect of LG25 either with combinational therapies or on drug resistance. Eradicating TNBC cells/tumors resistant to neoadjuvant chemotherapy is a critical unmet clinical need. Therefore, future research should be noted to test the effects of LG25 on drug-resistant TNBC cells in vitro or patient-derived xenograft

models, which might be effective models to see the reversal effect of LG25 against TNBC cells resistant to other apoptosis-inducing chemotherapy. In conclusion, our data reveal that LG25 is potentially an attractive therapeutic candidate for the treatment of TNBC.

## Abbreviations

Bax, B-cell lymphoma-2 (Bcl-2) associated X protein; BC, breast cancer; Bcl-2, B-cell lymphoma-2; CDC-2, cell division cycle protein 2; ER, estrogen receptor; FACS, fluorescence-activated cell sorter; FBS, fetal bovine serum; FITC, fluorescein isothiocyanate; HER2, human epidermal growth factor receptor 2; LG25, 5-(furan-2-carboxamido)-N-(4-(4-methylpiperazin-1-yl)phenyl)-1-(4-(trifluoromethyl)benzyl)-1H-indole-2-carboxamide; MDM-2, murine double minute 2; mTOR, mammalian target of rapamycin; NF- $\kappa$ B, nuclear factor kappa-light-chain-enhancer of activated B cells; PI, propidium iodide; PR, progesterone receptor; PTX, Paclitaxel; S6RP, S6 ribosomal protein; TNBC, triple-negative breast cancer.

## Availability Of Data And Material

All other data are included within the article and the [supplementary materials](#), or available from the authors on request.

## Acknowledgments

Financial support was provided by the Natural Science Foundation of Zhejiang Province (LY17B020008 to Z.L., LR18H160003 to Y.W., LY16H160050 to G.G.) for design of the study, collection, analysis and interpretation of data, and the National Natural Science Foundation of China (81750110549 to R.V. 81622043 to G.L.) for collection, analysis and interpretation of data, and writing of the manuscript.

## Author Contributions

G.G., G.L., and Y.W. participated in research design; X.X., V.R., Z.L., T.Y., and J.H. conducted experiments; S.S. and Z.L. contributed new reagents; X.X. and Y.W. performed data analysis; X.X. and Y.W. wrote the manuscript. All authors contributed to data analysis, drafting and revising the article, gave final approval of the version to be published, and agree to be accountable for the work.

## Disclosure

The authors report no conflicts of interest in this work.

## References

- Brenton JD, Carey LA, Ahmed AA, Caldas C. Molecular classification and molecular forecasting of breast cancer: ready for clinical application? *J Clin Oncol*. 2005;23(29):7350–7360. doi:10.1200/JCO.2005.03.3845
- Bianchini G, Balko JM, Mayer IA, Sanders ME, Gianni L. Triple-negative breast cancer: challenges and opportunities of a heterogeneous disease. *Nat Rev Clin Oncol*. 2016;13(11):674–690. doi:10.1038/nrclinonc.2016.66
- Balko JM, Giltman JM, Wang K, et al. Molecular profiling of the residual disease of triple-negative breast cancers after neoadjuvant chemotherapy identifies actionable therapeutic targets. *Cancer Discov*. 2014;4(2):232–245. doi:10.1158/2159-8290.CD-13-0286
- Liedtke C, Mazouni C, Hess KR, et al. Response to neoadjuvant therapy and long-term survival in patients with triple-negative breast cancer. *J Clin Oncol*. 2008;26(8):1275–1281. doi:10.1200/JCO.2007.14.4147
- Dent R, Hanna WM, Trudeau M, Rawlinson E, Sun P, Narod SA. Pattern of metastatic spread in triple-negative breast cancer. *Breast Cancer Res Treat*. 2009;115(2):423–428. doi:10.1007/s10549-008-0086-2
- Foulkes WD, Smith IE, Reis-Filho JS. Triple-negative breast cancer. *N Engl J Med*. 2010;363(20):1938–1948. doi:10.1056/NEJMra1001389
- Chin L, Gray JW. Translating insights from the cancer genome into clinical practice. *Nature*. 2008;452(7187):553–563. doi:10.1038/nature06914
- Molinari M. Cell cycle checkpoints and their inactivation in human cancer. *Cell Prolif*. 2000;33(5):261–274. doi:10.1046/j.1365-2184.2000.00191.x
- Hennessey BT, Smith DL, Ram PT, Lu Y, Mills GB. Exploiting the PI3K/AKT pathway for cancer drug discovery. *Nat Rev Drug Discov*. 2005;4(12):988–1004. doi:10.1038/nrd1902
- Kozaki K, Imoto I, Pimkhaokham A, et al. PIK3CA mutation is an oncogenic aberration at advanced stages of oral squamous cell carcinoma. *Cancer Sci*. 2006;97(12):1351–1358. doi:10.1111/j.1349-7006.2006.00343.x
- Wan X, Harkavy B, Shen N, Grohar P, Helman LJ. Rapamycin induces feedback activation of Akt signaling through an IGF-1R-dependent mechanism. *Oncogene*. 2007;26(13):1932–1940. doi:10.1038/sj.onc.1209990
- Liu P, Cheng H, Roberts TM, Zhao JJ. Targeting the phosphoinositide 3-kinase pathway in cancer. *Nat Rev Drug Discov*. 2009;8(8):627–644. doi:10.1038/nrd2926
- Costa RLB, Han HS, Gradishar WJ. Targeting the PI3K/AKT/mTOR pathway in triple-negative breast cancer: a review. *Breast Cancer Res Treat*. 2018;169(3):397–406. doi:10.1007/s10549-018-4697-y
- Gullett NP, Ruhul Amin AR, Bayraktar S, et al. Cancer prevention with natural compounds. *Semin Oncol*. 2010;37(3):258–281. doi:10.1053/j.seminoncol.2010.06.014
- Corsello MA, Kim J, Garg NK. Indole diterpenoid natural products as the inspiration for new synthetic methods and strategies. *Chem Sci*. 2017;8(9):5836–5844. doi:10.1039/c7sc01248a
- Wen H, Liu X, Zhang Q, et al. Three new indole diketopiperazine alkaloids from *Aspergillus ochraceus*. *Chem Biodivers*. 2018;15(4):e1700550. doi:10.1002/cbdv.201700550
- Liu Z, Tang L, Zhu H, et al. Design, synthesis, and structure–activity relationship study of novel indole-2-carboxamide derivatives as anti-inflammatory agents for the treatment of sepsis. *J Med Chem*. 2016;59(10):4637–4650. doi:10.1021/acs.jmedchem.5b02006
- Elinav E, Nowarski R, Thaïss CA, Hu B, Jin C, Flavell RA. Inflammation-induced cancer: crosstalk between tumours, immune cells and microorganisms. *Nat Rev Cancer*. 2013;13(11):759–771. doi:10.1038/nrc3611
- Dan HC, Cooper MJ, Cogswell PC, Duncan JA, Ting JP, Baldwin AS. Akt-dependent regulation of NF- $\kappa$ B is controlled by mTOR and Raptor in association with IKK. *Genes Dev*. 2008;22(11):1490–1500. doi:10.1101/gad.1662308

20. La Regina G, Coluccia A, Brancale A, et al. Indolylarylsulfones as HIV-1 non-nucleoside reverse transcriptase inhibitors: new cyclic substituents at indole-2-carboxamide. *J Med Chem.* 2011;54(6):1587–1598. doi:10.1021/jm101614j
21. Shattat G, Al-Qirim T, Sheikha GA, et al. The pharmacological effects of novel 5-fluoro-N-(9,10-dihydro-9,10-dioxoanthracen-8-yl)-1H-indole-2-carboxamide derivatives on plasma lipid profile of Triton-WR-1339-induced Wistar rats. *J Enzyme Inhib Med Chem.* 2013;28(4):863–869. doi:10.3109/14756366.2012.692085
22. Kuo CC, Hsieh HP, Pan WY, et al. BPR0L075, a novel synthetic indole compound with antimetabolic activity in human cancer cells, exerts effective antitumoral activity in vivo. *Cancer Res.* 2004;64(13):4621–4628. doi:10.1158/0008-5472.CAN-03-3474
23. Kaushik NK, Kaushik N, Attri P, et al. Biomedical importance of indoles. *Molecules.* 2013;18(6):6620–6662. doi:10.3390/molecules18066620
24. Singh AK, Bhadauria AS, Kumar U, et al. Novel Indole-fused benzoxazepines (IFBOs) inhibit invasion of hepatocellular carcinoma by targeting IL-6 mediated JAK2/STAT3 oncogenic signals. *Sci Rep.* 2018;8(1):5932. doi:10.1038/s41598-018-24288-0
25. El-Naga RN, Mahran YF. Indole-3-carbinol protects against cisplatin-induced acute nephrotoxicity: role of calcitonin gene-related peptide and insulin-like growth factor-1. *Sci Rep.* 2016;6:29857. doi:10.1038/srep29857
26. Bartholomeusz C, Gonzalez-Angulo AM. Targeting the PI3K signaling pathway in cancer therapy. *Expert Opin Ther Targets.* 2012;16(1):121–130. doi:10.1517/14728222.2011.644788
27. Cancer Genome Atlas N. Comprehensive molecular portraits of human breast tumours. *Nature.* 2012;490(7418):61–70. doi:10.1038/nature11412
28. Liu T, Yacoub R, Taliaferro-Smith LD, et al. Combinatorial effects of lapatinib and rapamycin in triple-negative breast cancer cells. *Mol Cancer Ther.* 2011;10(8):1460–1469. doi:10.1158/1535-7163.MCT-10-0925
29. Cossu-Rocca P, Orru S, Muroli MR, et al. Analysis of PIK3CA mutations and activation pathways in triple negative breast cancer. *PLoS One.* 2015;10(11):e0141763. doi:10.1371/journal.pone.0141763
30. Ooms LM, Binge LC, Davies EM, et al. The inositol polyphosphate 5-phosphatase PIPP regulates AKT1-dependent breast cancer growth and metastasis. *Cancer Cell.* 2015;28(2):155–169. doi:10.1016/j.ccell.2015.07.003
31. Liu H, Murphy CJ, Karreth FA, et al. Identifying and targeting sporadic oncogenic genetic aberrations in mouse models of triple-negative breast cancer. *Cancer Discov.* 2018;8(3):354–369. doi:10.1158/2159-8290.CD-17-0679
32. Moiseeva EP, Heukers R, Manson MM. EGFR and Src are involved in indole-3-carbinol-induced death and cell cycle arrest of human breast cancer cells. *Carcinogenesis.* 2007;28(2):435–445. doi:10.1093/carcin/bgl171
33. Sarkar FH, Li Y, Wang Z, Kong D. Cellular signaling perturbation by natural products. *Cell Signal.* 2009;21(11):1541–1547. doi:10.1016/j.cellsig.2009.03.009
34. Karin M. Nuclear factor-kappaB in cancer development and progression. *Nature.* 2006;441(7092):431–436. doi:10.1038/nature04870

## Drug Design, Development and Therapy

Dovepress

### Publish your work in this journal

Drug Design, Development and Therapy is an international, peer-reviewed open-access journal that spans the spectrum of drug design and development through to clinical applications. Clinical outcomes, patient safety, and programs for the development and effective, safe, and sustained use of medicines are a feature of the journal, which has also

been accepted for indexing on PubMed Central. The manuscript management system is completely online and includes a very quick and fair peer-review system, which is all easy to use. Visit <http://www.dovepress.com/testimonials.php> to read real quotes from published authors.

Submit your manuscript here: <https://www.dovepress.com/drug-design-development-and-therapy-journal>